Pramana – J. Phys. (2021) 95:189
https://doi.org/10.1007/s12043-021-02216-8

Role of γ–g band mixing in triaxial vs. deformed nuclei

J B GUPTA

Ramjas College, University of Delhi, Delhi 110 007, India
E-mail: jbgupta2011@gmail.com

MS received 4 June 2020; revised 27 June 2021; accepted 29 June 2021

Abstract. Recently, we illustrated the use of the γ–g absolute $B(E2)$ values in the Davydov–Filippov model (DFM), instead of the γ–g $B(E2)$ ratios, for analysing the spectral features of the ($\gamma < 20°$) deformed nuclei. Here, we illustrate the application of the absolute γ–g $B(E2)$ values to the triaxial ($\gamma > 20°$) nuclei to seek the new role of the γ variable in these nuclei, and to derive the underlying physics. The decrease of the absolute γ–g $B(E2)$ value for $\gamma > 20°$, instead of an increase observed for $\gamma < 20°$ deformed nuclei is explained. The increase of $B(E2, 2_\gamma - 0_1^+)$ in spite of the negative band mixing parameter, for deformed nuclei, reveals a new view of the band mixing angle, in contrast to its role for the triaxial nuclei. The three moment of inertia in DF model, for ^{158}Dy and ^{120}Xe display their degree of triaxiality.

Keywords. Nuclear structure; γ band; triaxiality; $B(E2)$.

PACS Nos 21.60.Ev; 21.10.Re; 27.70.+q

1. Introduction

The well-known Davydov–Filippov model (1958) [1] for the axially asymmetric deformed nuclei is an old, much cited model. On account of its simplicity, involving only a single parameter γ, for predicting the relative level energies and the $\gamma - g$ $B(E2)$ ratios, it has been used extensively over the last six decades, and it continues to be of interest. It is interesting to find what its basic merit is, and what are its limitations.

In an earlier study of the global application of the Davydov–Filippov model (DFM), to the collective motion in atomic nuclei, by Gupta and Sharma [2], it was noted that only the $B(E2, 2_\gamma - 0_1^+/2_1^+) = B1$ and $B(E2, 3_\gamma - 2_1^+/4_1^+) = B3$ ratios vary smoothly and monotonically with γ, in conformity with experiment. The other γ–g $B(E2)$ ratios for the $E2$ transitions from ($2_\gamma, 3_\gamma, 4_\gamma$) states exhibit secondary minimum/maximum at $\gamma \sim 20°$–$25°$, which are not supported in experiment in many instances.

It is well known [2,3] that at small values of γ ($< 15°$), the DF model predicts very high value of $K^\pi = 2^+$ γ-band, which is in disagreement with the experiment. The role of the moment of inertia about the longer axis is important here. Also the ground-state band level energies in DFM show little variation with asymmetry parameter γ ($0°-30°$), derived from the level energy ratio $R_\gamma = E(2_\gamma)/E(2_1^+)$.

Instead of using analytical expressions for the level energies and $B(E2)$ values suggested by Davydov and Filippov [1] for low spins, Liao Ji-Zhi [4] set up the nuclear Hamiltonian matrix, in terms of the moment of inertia expression of DFM, for studying low and higher spin states. In a two-state mixing set-up, Wood *et al* [5] gave a new meaning to the 2-state mixing angle τ between the inertia tensor and the electric tensor for the triaxial nuclei. Edmond *et al* [6] applied it to study the Os isotopes and for the evaluation of the three moments of inertia θ_k ($k = 1$–3) [7], from the experimental absolute $B(E2)$ values for spin $I^\pi = 2^+$ states. Gupta and Hamilton [8] applied the DF model for studying the unique spectral features of Ru isotopes. As the role of γ is important in general in different contexts, there is a need to extend these studies for a further understanding of the underlying physics.

In a recent study, Gupta [9] extended the work of ref. [2], to the DF predictions of the absolute $B(E2)$ values, wherein the role of γ for the axially symmetric well deformed ($\gamma < 20°$) nuclei was illustrated, which was not dealt with explicitly in earlier literature. That study revealed several unforeseen interesting features of the DF model, and illustrated its usefulness in predicting the variation of the spectral features of the

Published online: 08 November 2021

deformed nuclei with γ (0°–20°), in good agreement with experiment.

Since the values of the weak absolute γ–g $B(E2)$ values are often not available in experiment, one studies the $\gamma-g$ $B(E2)$ ratios which can be deduced from the γ-ray intensity I_γ branching ratios, and the $E2$ transition energies E_γ. However, in this procedure, often one misses the important role of the individual components of the $B(E2)$ ratio, thereby one may miss the underlying interesting physics.

To overcome the difficulty of getting absolute $B(E2)$ values for a given nucleus, the overall trend of the variation of the spectral features with varying γ were studied in [9], not for a comparison of the theory with experiment for the individual nucleus. This new approach seems to be valuable in understanding the essential role of γ in its own right, rather than the DF model serving merely as a reference model. In fact, it sets the simple one-parameter DF model as an essential and useful tool to study the important role of γ. While the variable β is a measure of the static deformation of a nucleus, γ plays a dynamic role in the fluctuation in β (or equivalently of γ) in a potential energy surface (PES) $V(\beta, \gamma)$ view.

In the present work, we study the role of γ, for the asymmetric deformed DF nuclei, also termed as rigid triaxial rotor (RTR) nuclei, to highlight the essential differences with the axially symmetric deformed nuclei. A clear partition of the full $\gamma(=$ 0–30°) space in two parts through the γ variable is enabled, which should be of immense interest. The different roles of the γ–g band mixing (and/or mixing angle τ [5]) in the two parts is illustrated. The anomaly of the increase of $B(E2, 2_\gamma - 0_1^+)$ for deformed non-DF nuclei in spite of the negative mixing angle [5] is explained. This reveals a wholly new physics.

In order to establish the basic physics of the DF or RTR model, we briefly review the RTR model in §2. In §3 the results from our analysis are given for the moment of inertia, level energies, and for the γ–g $B(E2)$ values and $B(E2)$ ratios. The role of the mixing angle τ as suggested by Wood *et al* [5] is reviewed for different values of γ. The application of the RTR model to compare the triaxiality in the deformed nucleus ^{158}Dy with the triaxial nucleus ^{120}Xe is illustrated. In §4, the summary and discussion are given.

2. The rigid triaxial rotor model or DFM

Davydov and Filippov [1] derived the expressions for the level energies and for the $\gamma-g$ $B(E2)$ values. In the energy unit of $\varepsilon = \hbar^2/4B\beta^2$,

$$E(2_i^+) = (9/X)(1 \pm Y), i = 2 \text{ or } 1 \tag{1}$$

where

$$X = \sin^2(3\gamma) \text{ and } Y = \sqrt{(1 - 8X/9)}.$$

The $B(E2)$s are expressed in the unit $(e^2 Q_0^2/16\pi)$, with $Q_0 = 3ZR^2\beta/\sqrt{5\pi}$ [1,2].

$$B(E2, 2_i^+ - 0_1^+) = 0.5\,[1 \pm (1 - 2X/3)/Y], i = 1 \text{ or } 2. \tag{2}$$

$$B(E2, 2_\gamma - 2_1^+) = (10/7)X/9Y^2. \tag{3}$$

For a given nucleus, the value of γ can be determined from the energy ratio

$$R_\gamma = E(2_\gamma)/E(2_1^+),$$

by using the expression (4) derived from (1)

$$X = \sin^2(3\gamma) = (9/8)[1 - (R_\gamma - 1)^2/(R_\gamma + 1)^2]. \tag{4}$$

Using the X and Y factors, $B(E2)$s can be evaluated. Alternatively, one may use

$$B2 = B(E2, 2_2^+ - 0_1^+)/B(E2, 2_1^+ - 0_1^+) = [Y - (1 - 2X/3)]/[Y + (1 - 2X/3)] \tag{5}$$

to determine X, Y and γ from the experimental value of $B2$.

The matrix method used by Wood *et al* [5] enables the determination of the mixing matrix element for γ, g band interaction. The model Hamiltonian may be expressed in terms of $A_k = 1/2\theta_k$ and the angular momentum operators J_i ($\hbar = 1$) [4,5].

$$H = A_1 J_1^2 + A_2 J_2^2 + A_3 J_3^2, \tag{6}$$

where the moment of inertia (irrotational) θ_k [$= \theta_0 \sin^2 (\gamma - 2\pi k/3)(k = 1, 2, 3)$, with $\theta_0 = 4B\beta^2$]. It may be rewritten in terms of the raising and lowering operators J_+ and J_- as

$$H = [AJ^2 + FJ_3^2] + G(J_+^2 + J_-^2) = H_0 + H_1, \tag{7}$$

where H_0 is diagonal. Here $A = (A_1 + A_2)/2$ and $F = A_3 - A$. The mixing parameter $G = (A_1 - A_2)/4$ is a measure of the triaxiality of the nucleus ($A_3 > A_2 > A_1$). For spin $I = 2$ state the (2×2) matrix is

$$\mathrm{H}(2) = \begin{vmatrix} 6A & 4\sqrt{3}G \\ 4\sqrt{3}G & 6A + 4F \end{vmatrix} \tag{8}$$

This yields [5]

$$E(2_i^+) = 6A + 2F \pm 2(F^2 + 12G^2)^{1/2}, \quad i = 2, 1, (2_2^+ = 2_\gamma). \tag{9}$$

Table 1. RTR values of inertial parameters A, F, G (in energy unit $\varepsilon = \hbar^2/4B\beta^2$), and mixing angle τ (in degree) as functions of γ.

γ	5°	10°	15°	20°	22°	25°	26°	28°	30°
A	0.68	0.71	0.77	0.86	0.91	1.01	1.05	1.14	1.25
F	65.2	15.9	6.70	3.41	2.65	1.79	1.55	1.13	0.75
G -ve	0.03	0.07	0.12	0.17	0.20	0.25	0.27	0.33	0.37
τ -ve	0.05	0.45	1.72	5.0	7.4	13.1	15.7	22.2	29.96
G/F	0.0005	0.004	0.018	0.05	0.075	0.14	0.17	0.29	0.49

In the 2-state mixing model, in the basis $|\text{IMK}\rangle$, the wave functions for $I = 2$ states ($K = 0, 2$) are given as [3]

$$|\psi_1\rangle = \alpha|2,\ K=0\rangle - \beta|2,\ K=2\rangle$$
$$|\psi_2\rangle = \beta|2,\ K=0\rangle + \alpha|2,\ K=2\rangle. \tag{10}$$

In terms of the mixing angle $\tau, \alpha = \cos\tau$ and $\beta = \sin\tau$, and

$$\beta/\alpha = \sin\tau/\cos\tau = \tan\tau = [(F^2 + 12G^2)^{1/2} - F)]/2\sqrt{3}G. \tag{11}$$

Wood *et al* [5] expressed the off-diagonal matrix element in terms of the mixing angle τ related to the factor G

$$2\sqrt{3}\,(G/F) = \tan 2\tau$$
$$B(E2, 2_\gamma - 0_1^+) = \sin^2(\gamma + \tau)$$
$$B(E2, 2_1^+ - 0_1^+) = \cos^2(\gamma + \tau) \tag{12}$$

and

$$\tan^2(\gamma + \tau) = B(E2, 2_\gamma - 0_1^+)/B(E2, 2_1^+ - 0_1^+) = B2. \tag{13}$$

The two versions of the model: as above are equivalent, if one employs the moment of inertia expressions of the triaxial rotor model. The option [5,7] of deriving the spectral features starting from the given ratio $B(E2, 2_\gamma - 0_1^+)/B(E2, 2_1^+ - 0_1^+) = B2$, is also illustrated in later sections.

3. Results

3.1 *Moment of inertia θ_k as a measure of triaxiality*

In DFM, the moment of inertia (MoI) $\theta_k = \theta_0 \sin^2(\gamma - 2\pi k/3)$, with $\theta_0 = 4B\beta^2$. For $\gamma = 0$ (axially symmetric nucleus), in the unit of θ_0, the moment of inertia $\theta_{1,2}$ about the two shorter axes are equal (0.75 each at $\gamma = 0$), and the MOI-3 $= \theta_3$ about the longer symmetry axis is zero. As γ is increased, MOI-2 θ_2 decreases, and MOI-3 θ_3 increases. The nucleus transforms from the axially symmetric prolate shape, via triaxial shape, towards the oblate shape (at $\gamma = 30°$).

3.2 *Inertial parameters of H_{RTR}*

Using the MoI expression (in unit of $\varepsilon = \hbar^2/4B\beta^2$), the inertial parameters A, F, G of eqs (6) and (7), for $\gamma = 5$–30° are given in table 1. The value of A varies rather slowly with varying γ, within a factor of 2. On the other hand, parameter F varies through a large factor. At small γ it varies fast (by a factor of 5 at $\gamma = 10°$ to 20° and also at $\gamma = 20°$ to 30°). The triaxiality parameter $G = (A_1 - A_2)/4$ increases significantly with γ, through a factor of three, for $\gamma = 15$–30°. In fact, the factor G/F and mixing angle τ increase significantly at $\gamma = 20$–30° for the DF nuclei. Note that here A, F and G are wholly dependent on γ. The dependence on the quadrupole deformation β and mass parameter B is through the scale unit ε.

Inserting A, F and G for varying values of γ in eq. (11), the mixing angle τ is determined as listed in table 1. For a given nucleus, γ can be obtained from the ratio R_γ of two energies, $E(2_\gamma)$ and $E(2_1^+)$ (or by any other procedure). Factor G/F is a measure of the band mixing.

3.3 *Interband γ–g absolute $B(E2)$*

The reduced $E2$ transition probability $B(E2, 2_\gamma - 0_1^+)$ plays the central role in the study of γ-band. It is a good measure of the γ–g band interaction. In units of $(e^2Q_0^2/16\pi)$, $[Q_0 = 3ZR^2\beta/\sqrt{(5\pi)}]$, it is given by eq. (2) in DFM, and by eq. (13) in the matrix method, as a function of the given γ. The results of the two procedures are found to be the same, if the expressions for triaxial MoI θ_k are used.

As depicted in figure 1, $B(E2, 2_\gamma - 0_1^+)$ vs. γ exhibits a peak at about $\gamma = 20°$. The rising part of this plot for $\gamma = 0°$–20° (applicable to the deformed nuclei) represents an interesting phenomenon. While increasing the value of γ, the intraband $B(E2, 2_1^+ - 0_1^+)$ value decreases (slightly) and the interband γ–g $B(E2, 2_\gamma - 0_1^+)$ value increases, for γ less than 20°, with a subsequent fall for larger γ up to $\gamma = 30°$. This is an unforeseen, but interesting result. In our previous study [9], it has been ascribed to the falling down of the 2_γ

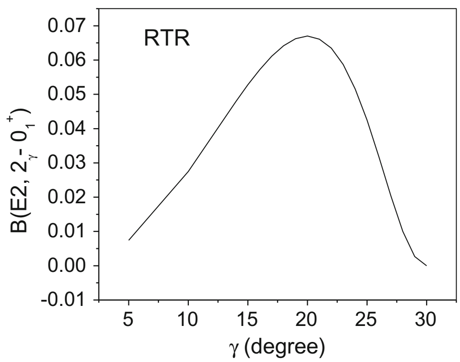

Figure 1. Plot of $B(E2, 2_\gamma - 0_1^+)$ vs. γ. A peak is formed at $\gamma = 20°$.

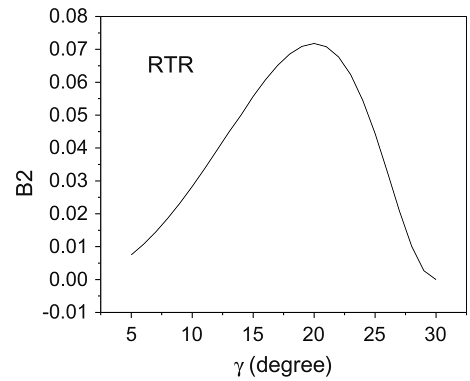

Figure 2. Plot of $B2$ vs. γ with a peak at $\gamma = 20°$.

state towards the ground band, with increasing value of γ. This gives rise to the increased γ–g interaction. But its effect on the γ–g $E2$ transition strength is different in the two regions: (i) the nuclei with γ less than $\sim$20° and (ii) the nuclei with γ more than 20°. The former set may be termed as non-DF and the latter set as the DF set of nuclei, or triaxial nuclei. As explained below, this difference reveals a wholly new view of the band mixing.

In the plot of $B(E2, 2_\gamma - 0_1^+/2_1^+)$ ratio only a smooth monotonic fall with increasing γ is exhibited [2,9]. For the absolute $B(E2, 2_\gamma - 0_1^+)$ value, the region of $\gamma = 0°$–$30°$ may be viewed in two parts, with different physics. While R_γ is used to determine the value of γ, the γ–g $B(E2, 2_\gamma^+ - 0_1^+)$ value is a good measure of the γ–g band interaction, playing a complementary role.

The seemingly γ-independent potential [10,11] in (β, γ) space for DF nuclei, does not convey the full view, because the equilibrium value of γ (or $\gamma_{\rm rms}$) varying between 20° and 30° determines the underlying physics.

An alternative entity $\Delta E = [E(2_\gamma) - E(4_1^+)]$ is also a good measure of this shape phase transition. For axially symmetric well deformed nucleus, ΔE is large. With increasing γ, ΔE decreases up to zero, when 2_γ crosses the 4_1^+ state ($R_\gamma = R_{4/2}$) [2,9], and for a larger γ (about $\gamma \sim 25°$), ΔE becomes negative. The 4_1^+ and 2_γ states form the members of the 2-phonon triplet for the anharmonic vibrator. So the value of ΔE is a measure of the transition from axially symmetric rotor to the asymmetric shape. Thus, it also determines the triaxiality. This entity in the microscopic view is related to the prolate–oblate potential energy surface (PES) minima difference $V_{\rm PO}$, as pointed out by Kumar [12].

3.4 *Interband to intraband $B(E2)$ ratio ($B2$)*

The interband to intraband $B(E2)$ ratio $B(E2, 2_\gamma - 0_1^+)/B(E2, 2_1^+ - 0_1^+) = B2$ (figure 2) depends on the asymmetry parameter γ (through X, Y factors, in eq. (5)). As intraband $B(E2, 2_1^+ - 0_1^+)$ in DFM (or matrix method), varies only by $\sim$7 %, on either side of the minimum (= 0.933 at $\gamma = 20°$) [9], the $B2$ curve (figure 2) is almost a replica of the $B(E2, 2_\gamma - 0_1^+)$ plot in figure 1. The $B2$ value at $\gamma = 20°$ of 0.718, the maximum value, as obtained by Wood *et al* [5], is obtained here $(0.067/0.933 = 0.718)$ in the irrotational flow assumption of DF model [1] as well. The $\sin^2(3\gamma) = X$ factor in eq. (5) enables this rise and fall of $B2$.

In physical terms, with increasing γ on the right side (figures 1 and 2), the 2_γ state moves down towards the ground band, and the decreasing $B(E2, 2_\gamma - 0_1^+)$ for $\gamma > 20°$ indicates increasing γ–g interference effects, unlike the process on the left side. The shape transition across the peak signifies the transition of the rotor symmetry to the anharmonic vibrator or γ-soft triaxial rotor regime. Both the wave functions and the $E2$ operator change. Now the selection rules of the phonon model or O(6) ($\Delta\sigma$, $\Delta\tau$ quantum numbers) will be applicable, rather than of the rotor model. Now, $B(E2, 2_\gamma - 0_1^+)$, the numerator in $B2$, signifies a $\Delta n = 2$ transition, resulting in the diminished $E2$ transition strength in the γ–g transitions.

For determining the mixing strength $\langle\psi|V|\psi\rangle$, one needs to put in the transition strength between the two levels involved from experiment [3,5]. The mixing strength is approximately equal to the ratio of mixing matrix elements, and the separation of the two unperturbed level energies (approximately equal to the observed separation) $= V/(E_2 - E_1)$ [3] (see last line of G/F) in table 1). Thus, the mixing strength depends upon two factors, the level separation (depending on the inertia tensor) and interaction strength V (depending on the $E2$ tensor). Wood *et al* suggested the use of $B(E2)$ ratio $B2$ for determining the values of γ [5]. Equation (5) can be solved for $X = \sin^2(3\gamma)$ and γ. For $\gamma = 0°$ or $30°(X = 0$ or $1)$, the numerator is reduced

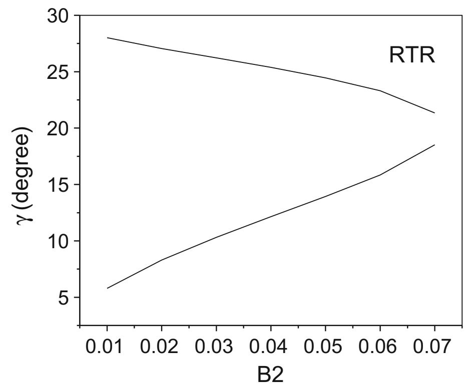

Figure 3. Plot of γ (degree) vs. $B(E2)$ ratio $B2$ in RTR model.

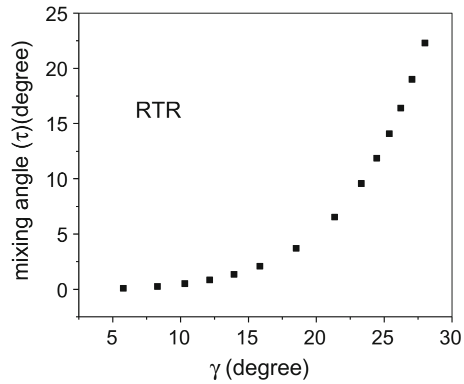

Figure 4. Plot of mixing angle τ (degree) vs. γ (degree) (from $B2$).

to zero, and a bell-shaped curve of $B2$ is expected *ab-initio*.

In table 2, the values of γ derived from the given $B2$ values are listed. Since it involves a sqrt factor, the solution from $B2$ for deriving γ involves squaring. The quadratic equation yields two values of γ, as listed in the first two rows of table 2 (also see figure 3). The first row values ($\gamma = 6°–19°$) (deformed rotors) (lower curve in figure 3) correspond to the left side of the $B2$ plot in figure 2, and the second row (21°–28°) (falling $B2$), corresponds to the right side of the plot (anharmonic vibrator or γ-soft rotor) (upper curve in figure 3). Also $\tan(\gamma + \tau) = (B2)^{1/2}$ (see eq. (13)) yields $(\gamma + \tau)$ (third row in table 2). The two values of mixing angle τ (last two rows) can be obtained by subtraction from the values of $(\gamma + \tau)$ and γ in the first two rows.

The plot of band mixing angle (τ) vs. γ (figure 4) illustrates the small, slow rising mixing angle τ for $\gamma = 5°–20°$ range, and faster rise for $\gamma = 20°–30°$. The lower part of the curve corresponds to the left side of the rising $B(E2, 2_\gamma - 0_1^+)$ (figure 1) and of $B2$ (figure 2), and the second part corresponds to the right side of these plots.

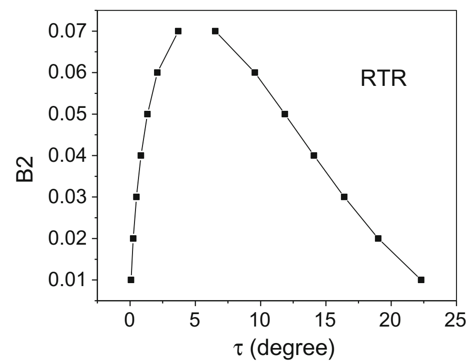

Figure 5. Plot of ratio $B2$ vs. mixing angle τ.

It is interesting to note that, in spite of the negative mixing angle τ, in both parts, of the $B2$ curve, it is surpassed by the larger positive band interaction, giving rise to increasing $B(E2, 2_\gamma - 0_1^+)$ and $B2$ in the first part, applicable to the deformed nuclei, as noted above. This special situation should be of general interest, not recognised before. The destructive interference referred to in [5], is effective indeed for the DF nuclei, where DF or RTR model is usually applied. Thus, the present study offers an extension to the novel work of Wood *et al* [5].

It is interesting to view the variation of the mixing angle τ for varying $B2$. The plot of $B2$ vs. the mixing angle yields the bell-shaped curve (figure 5). It reinforces the above argument for the deformed nuclei. $B2$ rises sharply, when the negative mixing angle due to destructive interference (of the off diagonal term) is rather small (0°–6°). Obviously, some other process is involved, as cited above, the falling of γ band closer to ground band for the deformed rotor regime.

As discussed already, the difference of 2_γ and $4_1^+ = \Delta E$ is important here. Smaller the ΔE, the greater is the anharmonicity or the γ-softness. Thus, the $B(E2, 2_\gamma - 0_1^+)$ and $B2$ curves explain the changing physics here. The large value of the mixing angle τ close to $\gamma = 30°$ has to be viewed in terms of the changing selection rules, besides a large mixing of γ and ground bands. Wood *et al* ascribed it to the destructive interference effect [5].

3.5 *Novel method to deduce moment of inertia – example*

Consider the application of the RTR model to the deformed nucleus ^{158}Dy, and the triaxial nucleus ^{120}Xe, as examples of the two sets of nuclei (see table 3).

$B(E2)$ EXP value is in e^2b^2, and the DFM value is in unit of $(e^2Q_0^2/16\pi)$ (see text for normalised value in e^2b^2), using the values of $B(E2, 2_1^+ - 0_1^+)$ in EXP and DFM.

Table 2. γ (degree) from $B2$ using eq. (5) (upper and lower rows) correspond to the two branches of $B2$ in figure 2. Third row is for $\tan(\gamma+\tau)=\sqrt{(B2)}$ (eq. (13)). $D1(-)\tau$, $D2(-)\tau$ are by subtraction.

$B2$	0.01	0.02	0.03	0.04	0.05	0.06	0.07
γ	5.79°	8.30°	10.32°	12.15°	13.94°	15.85°	18.52°
γ	28.01°	27.06°	26.23°	25.39°	24.46°	23.32°	21.35°
$\gamma+\tau$	5.71°	8.05°	9.82°	11.31°	12.60°	13.76°	14.82°
$D1(-)\tau$	0.08°	0.25°	0.50°	0.84°	1.34°	2.09°	3.70°
$D2(-)\tau$	22.30°	19.01°	16.41°	14.08°	11.86°	9.56°	6.53°

In table 3, the $B(E2)$ value in DFM are in the unit of $[(e^2Q_0^2/16\pi), Q_0=3ZR^2\beta/\sqrt{(5\pi)}]$, while the experimental values are in e^2b^2. For a comparison with the experimental data, the unit for $B(E2)$ in DFM needs to be normalised using experimental $B(E2, 2_1^+-0_1^+)$. The slow variation of the intraband $B(E2, 2_1^+-0_1^+)$ in the ground band with varying γ, changes little. Note that the sum $B(E2, 2_1^+-0_1^+)+B(E2, 2_\gamma-0_1^+)$ in DFM is equal to 1.00 unit.

If we normalise $B(E2, 2_\gamma-0_1^+)$ to experimental $B(E2, 2_1^+-0_1^+)$ in ^{158}Dy, it will reduce to 0.041 e^2b^2. Similarly, in ^{120}Xe, it will reduce from 0.056 to 0.029 e^2b^2, in better agreement with the experimental value of 0.020 e^2b^2.

For the deformed nucleus ^{158}Dy, with $R_\gamma=9.57$ and $\gamma=12.8°$, the DF model yields $B2=0.044$ and the mixing angle $\sim 1.0°$. It lies on the left side of the peak in figure 2. The mixing angle τ agrees with the values of τ listed in table 1, derived from the given γ values, after interpolation. It also agrees with the values in table 2, listing γ and τ derived from the given $B2$ values after interpolation. But the predicted value of $B2=0.044$ deviates from the experimental value of 0.032(2). The deviation of DF values of $B2$ from the experimental values was noted by Wood *et al* [5] in their global plot of $B2$ vs. R_γ. It is a regular feature of the DF model predictions of $B(E2)$. It represents the effect of γ derived from R_γ, or the effect of the moment of inertia based on expressions in DF model.

To avoid the problems associated with the use of irrotational moment of inertia, Almond and Wood [7] suggested the use of expressions based on the experimental energies of 2_1^+, 2_γ, and of the $B2$ ratio for a given nucleus, instead of deriving it from the RTR model, using R_γ and γ. While unit of energy cancels out in the ratio R_γ, in the sum and difference method of ref. [7], one retains the unit of MeV (or keV). This is a novel innovation, suggested by Almond and Wood [7]. The values of A, F and G can be evaluated from eq. (9), using the sum and difference of experimental values of $E(2_\gamma)$ and $E(2_1^+)$, and $B2$. Then the moment of inertia θ_k can be determined from the following expressions:

$$A+2G=1/2\theta_1,$$
$$A-2G=1/2\theta_2,$$
and
$$A+F=1/2\theta_3. \tag{14}$$

For ^{158}Dy, using the above procedure, for $B(E2, 2_\gamma-0_1^+)=0.030$ we get the value of γ as 10.7° instead of 12.8° obtained from R_γ (in table 3). This difference in the value of γ represents the deviation of the calculated $B2$ values in the plot of $B2$ vs. R_γ, illustrated by Wood *et al* [5], in general, for the deformed region.

By increasing the value of $B(E2, 2_\gamma-0_1^+)$ from 0.030 to 0.035, a rise of 2σ (measure of error limit), γ rises to 11.7°, nearer to the value from R_γ. The effect on the deduced MoI is less. From this we learn that the improved method of ref. [7] will be useful, if one gets the $B(E2, 2_\gamma-0_1^+)$ value from Coulomb excitation experiment or other methods, with sufficient accuracy (say, within 20%), with a corresponding uncertainty ($\sim$10%) in the prediction of γ and less uncertainty in MoI values.

Thus, the novel method of ref. [7] is useful to give a glimpse in the degree of triaxiality of a nucleus, in addition to what one can learn from the usual derivation of MoI (θ_k) as discussed in §3.1. For ^{158}Dy, the predicted values of MoI are 35, 26 and 2 MeV^{-1} for $B2=0.30$ e^2b^2, and 37, 25 and 2 MeV^{-1} for $B2=0.35$ e^2b^2.

^{120}Xe with $R_\gamma=2.720$ and $\gamma=23.4°$ (table 3) is an example of a triaxial nucleus. In the DF model [1] or the matrix method [4,5], we get $B2=0.60$ compared to the experimental value of 0.40. The mixing angle $\tau=9.7°$ (table 3) is much larger than the value obtained for the deformed nucleus ^{158}Dy. Based on the experimental $B2$ value, in the method of ref. [7], the mixing angle increases to 14.1° (table 4). This reflects the relation of $B2$ with γ on the right side of the $B2$ curve (figure 2).

Note that 2_γ is now closer to 2_1^+ (or 4_1^+), and the band mixing effect on the two sides of the bell-shaped $B2$ curve is different, as we discussed above for the deformed nuclei. Here, for the triaxial nuclei, the interpretation in [5], of the destructive effect of the off-diagonal interference term holds good.

Table 3. Energies in keV, γ and τ in degree. See text for unit of $B(E2)$.

	$E(2_1^+)$	$E(2_\gamma)$	R_γ	γ	$B(E2_1^+ - 0_1^+)$	$B(E2, 2_\gamma - 0_1^+)$	$B2$	τ
^{158}Dy EXP	98.9	946.3	9.57	12.8°	0.934	0.030(2)	0.032(2)	
DFM					0.958	0.042[a]	0.044	1.0°
^{120}Xe EXP	322.6	876.1	2.720	23.4°	0.500	0.020(2)	0.040(2)	
DFM					0.944	0.056[a]	0.059	9.7°

Table 4. Level energy (MeV), $B(E2, I_i - I_f)$ (e^2b^2), other factors and MoI (MeV)$^{-1}$.

Ist row 2nd row	$E(2_1^+)$ $\theta_k, k = 1$	$E(2_2^+)$ 2	$(2_1^+ - 0_1^+)$ 3	$(2_\gamma - 0_1^+)$	γ	τ	F	A	G
^{158}Dy	0.099	0.946	0.934	0.030	10.7°	−0.57°	0.212	0.017	−0.0012
MoI θ_k	35.4	26.5	2.19						
^{158}Dy				0.035	11.7°	−0.74°	0.212	0.017	−0.0016
MoI θ_k	37.4	25.4	2.19		–				
^{120}Xe	0.322	0.876	0.50	0.020	25.4°	−14.1°	0.122	0.059	−0.0189
MoI θ_k	23.4	5.2	2.8						

Values of θ_k ($k = 1$–3) of 23.4, 5.2 and 2.8 MeV^{-1} for ^{120}Xe (table 4) reflect the increased triaxiality, with θ_1 remaining high and θ_2 nearing closer to θ_3.

The bell-shaped curve of $B2$ in the DF model represents this difference of the two nuclei. Also $B(E2, 2_\gamma - 0_1^+/2_1^+)$ ratio $= B1$ is only 0.039(4) for ^{120}Xe, compared to 0.30(4) for ^{158}Dy, so that, the former lies at the bottom of the $B1$ vs. γ plot, while the latter lies much higher towards the Alaga value of 0.7.

4. Summary and discussion

Figures 1 and 2 display the bell-shaped curves of $B(E2, 2_\gamma - 0_1^+)$ and $B2$ respectively, with a peak at $\gamma = 20°$, which implies their rise with increasing γ up to $\gamma = 20°$ and a fall for $\gamma > 20°$. The entity $\Delta E = [E(2_\gamma) - E(4_1^+)]$, a measure of the separation of γ-band from the ground band, affects the γ–g interaction. Up to a certain value, the band interaction corresponds to the growth in the left part of the bell-shaped curve, and falling value beyond it corresponds to the right part of the peak. This is interesting and needs a deeper analysis.

In the plot of γ vs. $B2$ (figure 3), the lower curve indicates increasing γ for the full range of $B2$. The upper curve corresponds to the decreasing $B2$, for increasing γ beyond 20°. This confirms the view in figure 2. The plot of mixing angle τ vs. γ (figure 4) indicates slow rise of τ for small γ (say up to 20°), and a faster rise beyond it. The band mixing is small in the first part, corresponding to the deformed nuclei. Same physics is evident in the plot of $B2$ vs. mixing angle τ (figure 5), viz. fast rise of $B2$ for small τ, and slow fall of $B2$ for larger value of τ. From all these findings, it is evident that the increase of $B(E2)$ or $B2$ in the left part of figures 1 and 2 involves a physics which is different from its fall in the right part. The wave functions and selection rules for the two parts are different. From the present study, the merits of DFM and its limitations are illustrated, and the functional role of γ is made more transparent.

Acknowledgements

The author appreciates the post-retirement association with Ramjas College.

References

[1] A S Davydov and G F Filippov, *Nucl. Phys.* **8**, 237 (1958)
[2] J B Gupta and S Sharma, *Phys. Scr.* **39**, 50 (1989)
[3] R F Casten, *Nuclear structure from a simple perspective* (Oxford University Press, 1990)
[4] L Ji-Zhi, *Phys. Rev. C* **51**, 141 (1995)
[5] J L Wood, A M Oros-Peusquens, R Zaballa, J M Almond and W D Kulp, *Phys. Rev. C* **70**, 024308 (2004)
[6] J M Edmond, R Zabella, A M Oros-Peusquens, W D Kulp and J L Wood, *Phys. Rev. C* **78**, 014302 (2008)
[7] J M Almond and J L Wood, *Phys. Lett. B* **767**, 225 (2017)
[8] J B Gupta and J H Hamilton, *Eur. Phys. J. A* **56**, 14 (2020)
[9] J B Gupta, *Int. J. Mod. Phys. E* **29**(**6**), 2050037 (2020)
[10] L Wilets and M Jean, *Phys. Rev.* **102**, 788 (1956)
[11] J B Gupta, *Eur. Phys. J. A* **55**, 122 (2019)
[12] K Kumar, *Phys. Rev. C* **1**, 1 (1970)